ADVANCED MATERIALS

[15] a) K. Matsuda, M. Irie, *Chem. Lett*. **2000**, 16. b) K. Matsuda, M. Irie, *J. Am. Chem. Soc.* **2000**, *122*, 7195. c) K. Matsuda, M. Matsuo, S. Mizoguti, K. Higashiguchi, M. Irie, *J. Phys. Chem.* **2002**, *106*, 11 218.

[16] a) S. Fraysse, C. Coudret, J. P. Launay, *Eur. J. Inorg. Chem.* **2000**, 1581. b) J. M. Endtner, F. Effenberger, A. Hartschuh, H. Port, *J. Am. Chem. Soc.* **2000**, *122*, 3037.

[17] a) M. Irie, K. Uchida, T. Eriguchi, H. Tsuzuki, *Chem. Lett.* **1995**, 899. b) S. Kobatake, K. Uchida, E. Tsuchida, M. Irie, *Chem. Commun.* **2002**, 2804. c) S. Yamamoto, K. Matsuda, M. Irie, *Angew. Chem. Int. Ed.* **2003**, *42*, 1636. d) S. Kobatake, M. Irie, *Bull. Chem. Soc. Jpn.* **2004**, *77*, 195.

[18] a) T. Kawai, T. Koshido, K. Yoshino, *Appl. Phys. Lett.* **1995**, *67*, 795. b) T. Koshido, T. Kawai, K. Yoshino, *Jpn. J. Appl. Phys., Part 2* **1995**, *34*, L389. c) T. Kawai, T. Koshido, Y. Kaneuchi, K. Yoshino, *Thin Solid Films* **1996**, *273*, 195.

[19] a) N. Tanio, M. Irie, *Jpn. J. Appl. Phys., Part 1* **1994**, *33*, 1550. b) N. Tanio, M. Irie, *Jpn. J. Appl. Phys., Part 1* **1994**, *33*, 3942. c) F. Ebisawa, M. Hoshino, K. Sukegawa, *Appl. Phys. Lett.* **1994**, *65*, 2919.

[20] a) H. Nakashima, M. Irie, *Macromol. Rapid Commun*. **1997**, *18*, 625. b) H. Nakashima, M. Irie, *Macromol. Chem. Phys.* **1999**, *200*, 683.

[21] J. Biteau, F. Chaput, K. Lahlil, J. P. Boilot, G. M. Tsivgoulis, J. M. Lehn, B. Darracq, C. Marois, Y. Levy, *Chem. Mater*. **1998**, *10*, 1947.

[22] a) T. Kawai, N. Fukuda, D. Mayer, S. Kobatake, M. Irie, *Jpn. J. Appl. Phys., Part 2* **1999**, *38*, L1194. b) M.-S. Kim, T. Kawai, M. Irie, *Mol. Cryst. Liq. Cryst.* **2000**, *345*, 251. c) M.-S. Kim, T. Kawai, M. Irie, *Chem. Lett.* **2000**, 1188. d) M. S. Kim, H. Maruyama, T. Kawai, M. Irie, *Chem. Mater.* **2003**, *15*, 4539.

[23] E. Kim, Y.-K. Choi, M. H. Lee, *Macromolecules*, **1999**, *32*, 4855.

[24] T. Tsujioka, Y. Hamada, K. Shibata, A. Taniguchi, T. Fuyuki, *Appl. Phys. Lett.* **2001**, *78*, 2282.

[25] A. Peters, R. McDonald, N. R. Branda, *Chem. Commun*. **2002**, 2275.

[26] T. Kawai, T. Iseda, M. Irie, *Chem. Commun.* **2004**, 72.

[27] a) L. N. Luca, J. J. D. de Jong, J. H. van Esch, R. M. Kellogg, B. L. Feringa, *Eur. J. Org. Chem.* **2003**, 155. b) J. J. D. de Jong, L. N. Lucas, R. Hania, A. Pugzly, R. M. Kellogg, B. L. Feringa, K. Duppen, J. H. van Esch, *Eur. J. Org. Chem.* **2003**, 1887.

[28] K. Yoshino, K. Tada, K. Yoshimoto, M. Yoshida, T. Kawai, H. Araki, M. Hamaguchi, A. Zakhidov, *Synth. Met.* **1996**, *78*, 301.

[29] a) T. Tsujioka, H. Kondo, *Appl. Phys. Lett*. **2003**, *83*, 937. b) T. Tsujioka, K. Masuda, *Appl. Phys. Lett.* **2003**, *83*, 4978.

[30] D. Dulic, S. J. van der Molen, T. Kudernac, H. T. Jonkman, J. J. D. de Jong, T. N. Bowden, J. van Esch, B. L. Feringa, B. J. van Wees, *Phys. Rev. Lett.* **2003**, *91*, 207 402.

[31] T. Kawai, T. Kunitake, M. Irie, *Chem. Lett.* **1999**, 905.

[32] F. Stellacci, C. Bertarelli, F. Toscano, M. C. Gallazzi, G. Zotti, G. Zerbi, *Adv. Mater.* **1999**, *11*, 292.

[33] a) A. Peters, N. R. Branda, *Adv. Mater. Opt. Electron.* **2000**, *10*, 245. b) T. Kaieda, S. Kobatake, H. Miyasaka, M. Murakami, N. Iwai, Y. Nagata, A. Itaya, M. Irie, *J. Am. Chem. Soc.* **2002**, *124*, 2015.

[34] S. Kobatake, M. Irie, *Tetrahedron* **2003**, *59*, 8359.

[35] For syntheses, characterization of compounds, ^{1}H NMR data, fluorescence, and GPC profiles, see Supporting Information.

[36] M. Irie, K. Sakemura, M. Okinaka, K. Uchida, *J. Org. Chem.* **1995**, *60*, 8305.

[37] R. M. Metzger, T. Xu, I. Peterson, *J. Phys. Chem., B* **2001**, *105*, 7280.

[38] G. A. Kossmehl, in *Handbook of Conducting Polymers*, Vol. 1, 1st ed. (Ed: T. A. Skotheim), Marcel Dekker, New York **1986**, Ch. 10.

[39] J. Su, W. D. Wulff, R. G. Ball, *J. Org. Chem.* **1998**, 63, 8440.

[40] K. Orito, T. Hatakeyama, M. Takeo, H. Suginome, *Synthesis* **1995**, *10*, 1273.

[41] Q. Hou, Y. Xu, W. Yang, M. Yuan, J. Peng, Y. Cao, *J. Mater. Chem.* **2002**, *12*, 2887.

Enzymatic Synthesis and Nanostructural Control of Gallium Oxide at Low Temperature**

By *David Kisailus*, *Joon Hwan Choi*, *James C. Weaver*, *Wenjun Yang*, and *Daniel E. Morse**

The molecular mechanisms underlying the biological synthesis of nanostructured mineral/organic composites have long been recognized to offer exciting prospects for materials science.[1–8] In addition to their benign conditions for synthesis (including neutral pH, low temperature, low pressure, and the absence of caustic chemicals), these mechanisms often reveal a precision of nanostructural control not yet achievable in anthropogenic syntheses. Investigations into such mechanisms have shown that protein filaments occluded within the silica skeletal elements of a marine sponge consist of structure-directing enzymes capable of catalyzing, in vitro, the hydrolysis and polycondensation of molecular precursors of silica, silsesquioxanes,[5,9–11] and titania.[12] We show here that these protein filaments are not only capable of the hydrolysis and polycondensation of a gallium oxide molecular precursor to yield (depending on the reaction conditions) either gallium oxo-hydroxide (GaOOH) or spinel gallium oxide (γ-Ga_2O_3, a gas-sensing semiconductor) at room temperature, but also to direct their resulting structures. This control is seen in the defined orientation of nanocrystals with respect to the surface of the protein, suggesting that structural determinants on the surface of the protein catalyze the formation of the γ-Ga_2O_3 polymorph at low temperatures and may direct its crystallographic orientation. These results demonstrate the feasibility of a low-temperature catalytic route to the synthesis and

[*] Prof. D. E. Morse, Dr. D. Kisailus, J. C. Weaver, Dr. W. Yang
Materials Research Laboratory and
Institute for Collaborative Biotechnologies and
the California NanoSystems Institute
University of California
Santa Barbara, CA 93106-9610 (USA)
E-mail: d_morse@lifesci.ucsb.edu
Prof. D. E. Morse
Department of Molecular, Cellular, and Developmental Biology
Marine Science Institute
University of California
Santa Barbara, CA 93106-9610 (USA)
Dr. J. H. Choi
Materials Research Laboratory
University of California
Santa Barbara, CA 93106-9610 (USA)

[**] We thank Professor Tzi Sum Andy Hor (National University of Singapore) for his insightful suggestions. This work was supported by grants from the U.S. Dept. of Energy (DE-FG03-02ER46006), NASA (NAG1-01-003 and NCC-1-02037), the Institute for Collaborative Biotechnologies through grant DAAD19-03D-0004 from the U.S. Army Research Office, the NOAA National Sea Grant College Program, U.S. Department of Commerce (NA36RG0537, Project R/MP-92) through the California Sea Grant College System, and the MRSEC Program of the National Science Foundation under award No. DMR-96-32716 to the UCSB Materials Research Laboratory.

  DOI: 10.1002/adma.200400815

nanostructural control of metal oxide semiconductors in a biologically inspired process formally analogous to current metal-organic chemical vapor deposition (MOCVD) technology.

Investigation of the mechanisms governing the biological synthesis of silica structures in a marine sponge (*Tethya aurantia*) led to the surprising discovery that this synthesis is mediated, in part, by a family of catalytically active, structure-directing enzymes[5,9–12] containing the catalytic triad (serine, histidine, and asparagine residues) typical of a large family of hydrolases.[13] Silica needle-like skeletal elements (spicules) made by *T. aurantia* each contain an axial protein filament, comprised primarily of three highly similar subunits called silicateins, that spatially directs the deposition of silica along its entire length. The intact protein filaments and their constituent monomers obtained from disaggregation of the filaments, and those produced from recombinant DNA templates cloned in bacteria, were shown in vitro to catalyze the hydrolysis and structurally direct the polycondensation of silicon and organosilicon alkoxides to yield silica and polysilsesquioxanes (silicones) at neutral pH.[9,10,14]

Genetic engineering verified the essential requirement for the principal residues of the catalytic site of the silicateins, supporting a mechanism of action closely related to that of the well-known hydrolases.[11] Predictive synthesis of biomimetic diblock copolypeptides based on this result yields catalytically active molecules that exhibit both silica-polymerizing and structure-directing capabilities.[15] We recently found that the silicatein filaments can be used to catalyze the synthesis of titanium dioxide from a stable molecular precursor.[12] This mechanism can be harnessed for nanostructural control of gallium oxide, a semiconductor with optoelectronic and gas-sensing applications.[16,17]

To test the possibility that silicatein filaments can catalyze the hydrolysis of a main-group metal complex (hydrated gallium(III) nitrate, GNO) with subsequent polycondensation to yield product in quantity sufficient for characterization by X-ray diffraction (XRD), we first examined the reaction of silicatein filaments with an aqueous solution of highly concentrated GNO at 16 °C (Fig. 1).

Under these conditions, silicatein filaments were observed to promote the hydrolysis of the starting material and subsequent polycondensation to form GaOOH (Fig. 1a). This is the first reported example of which we are aware in which this material has been formed at low temperature, from a water-soluble precursor, in the absence of added acid or alkali. Under the same conditions, silicatein filaments that had first been denatured at high temperature were inactive (Fig. 1b), proving that the reaction observed was dependent upon the integrity of the three-dimensional structure of the native protein. A similar requirement previously had been observed for the low-temperature formation of silica and silsesquioxanes from the corresponding silicon alkoxides by silicatein at neutral pH.[10,11] Proof that silicatein catalyzed the hydrolysis of GNO was seen in the observed reduction in pH of the starting solution in the presence of the native protein, and the absence

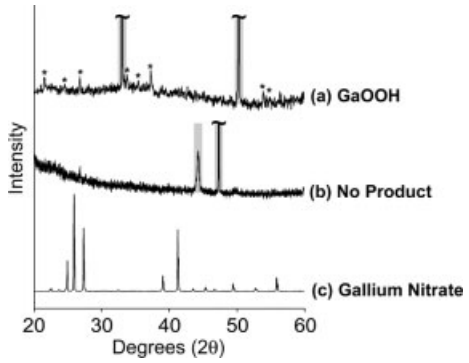

Figure 1. a) GaOOH product (highlighted by asterisks) formed from 1.0 M gallium nitrate by catalysis and templating by native silicatein filaments at 16 °C; b) absence of product with heat-denatured silicatein filaments; and c) gallium nitrate (starting precursor). (Gray bars indicate Si internal-standard peaks.)

of any change in pH when the denatured protein was used (data not shown). The behavior of the GNO precursor in aqueous media is quantitatively explained by the Partial-Charge Model (PCM)[18] that considers the partial charges on the metal cation and its ligands at electronic equilibrium. PCM calculations for the GNO–H_2O system predict that hydration is thermodynamically favored over spontaneous hydrolysis under the acidic conditions of our experiments, thus explaining the stability of the complex and the requirement for catalysis of the hydrolysis that we observe.

To examine the possible relationship between the surface of the silicatein filament and the reaction product formed from GNO under kinetically constrained conditions, lower precursor and silicatein concentrations were used while maintaining the original precursor/silicatein molar ratio. Under these conditions, a reaction product was formed as a dispersed coating of nanocrystallites (75–200 nm diameter) adhering to the surfaces of the silicatein filaments (Fig. 2a).

When heat-denatured filaments were used, no reaction product was observed (Fig. 2b). Energy dispersive spectroscopy (EDS) measurements of the oxide-coated filament indicated the presence of both gallium and oxygen (data not shown). EDS confirmed the absence of gallium from the heat-denatured protein surface after the 24 h reaction time. Silk fibers incubated with the GNO solution under identical conditions also exhibited no coating on their surfaces after 24 h (Fig. 2c). Although at low GNO concentration sufficient product for analysis by XRD was not obtained, analysis by high-resolution transmission electron microscopy and selected area diffraction (Fig. 3) revealed that the nanocrystallites had *d*-spacings (±0.02 Å) of 2.91 Å, 2.48 Å, 2.08 Å, 1.44 Å, and 1.20 Å corresponding to the (220), (311), (440), (400), and (533) planes, respectively, of cubic γ-Ga_2O_3, a spinel polymorph typically formed at high temperatures (> 400 °C).

Diffraction revealed that these nanocrystallites exhibited a preferred orientation relative to the principal fiber axis of the macroscopic silicatein filaments. Independent analyses of nine crystals on different filaments gave the same results. The

ADVANCED MATERIALS

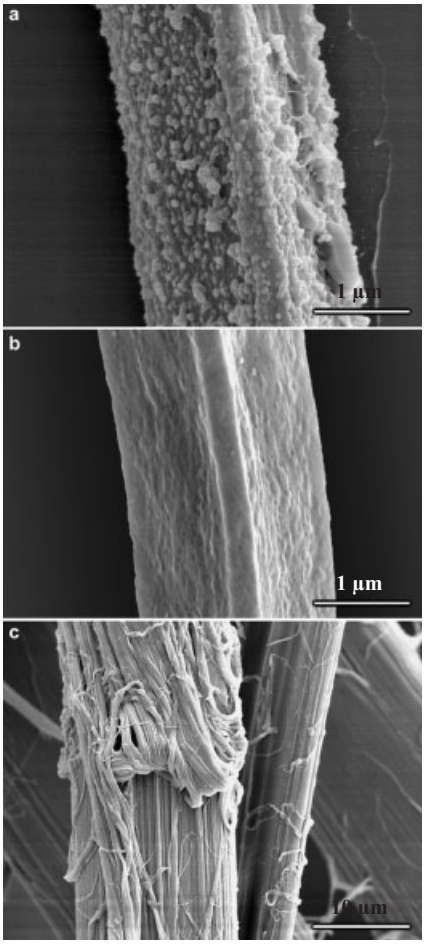

Figure 2. a) Ga_2O_3 product formed from 0.1 M gallium nitrate by catalysis and templating by native silicatein filaments at 25 °C; absence of product with b) denatured silicatein filaments and c) silk fibers.

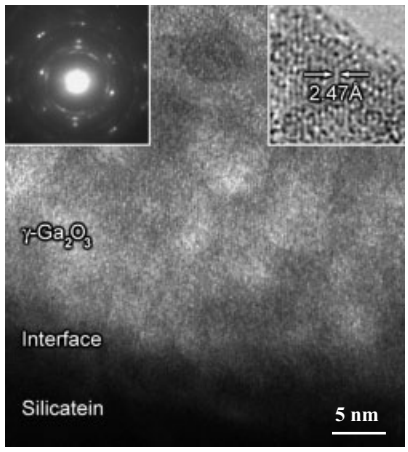

Figure 3. Lattice fringes of the oxygen-rich (311) planes of oriented Ga_2O_3 formed from gallium nitrate by catalysis and templating with silicatein. Insert, upper left: Selected area electron diffraction pattern showing that γ-Ga_2O_3 particles formed by silicatein catalysis are single crystals with (311) planes preferentially oriented relative to the surface of silicatein filaments. Insert, upper right: Expanded view of lattice fringes.

(311) planes of the oxide nanocrystals were oriented nearly perpendicular to (86.44° ± 2.84°) the surface of the filament. The *d*-spacing of the lattice fringes seen in Figure 3 was measured at 2.47 ± 0.02 Å, consistent with the diffraction data and corresponding to (311) γ-Ga_2O_3. These results suggest that the silicatein surface may have directed the growth of the condensation product in a pseudo-epitaxial manner, favoring the orientation of specific gallium oxide planes with respect to the protein surface. In contrast, our attempts to synthesize γ-Ga_2O_3 from GNO solutions at low temperature by addition of alkali in the absence of a templating surface were unsuccessful, yielding only gallium oxo-hydroxide (Fig. 4c). Heating

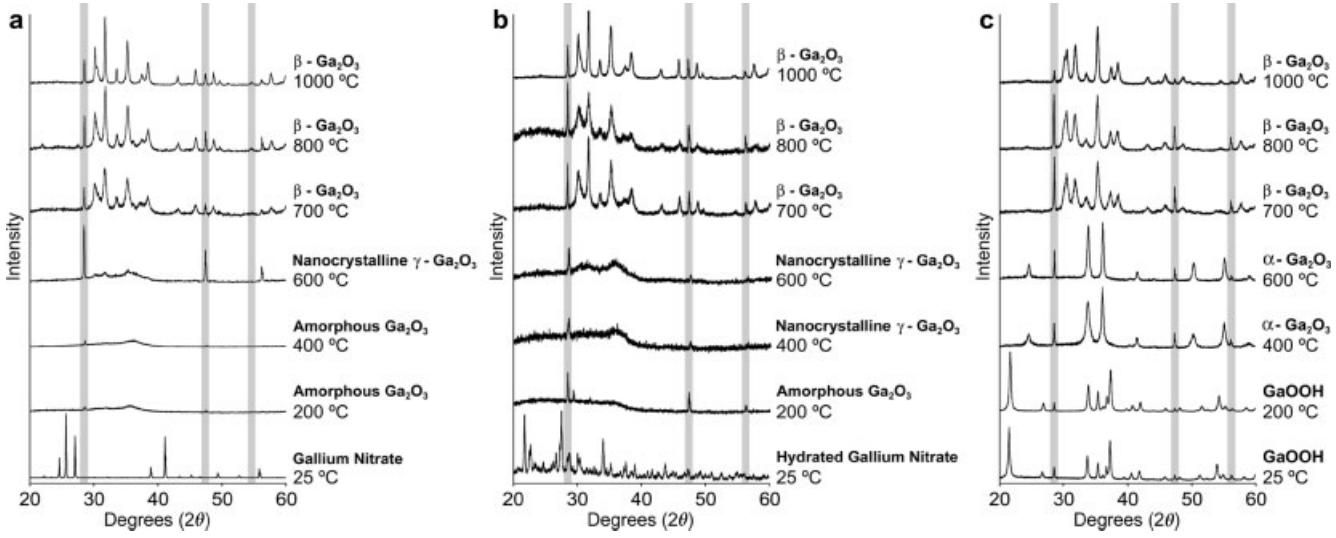

Figure 4. Temperature dependent phase transformations yielding Ga_2O_3 powders from dehydration and pyrolysis of: a) gallium nitrate; b) hydrated gallium nitrate; and c) GaOOH obtained from (a) by alkali hydrolysis. (Gray columns indicate peaks of the internal Si standard.)

above ca. 250 °C under dynamic vacuum was required to dehydrate the oxo-hydroxide.

Investigation of the thermal dehydration and decomposition of various gallium nitrate-based precursors of crystalline gallium oxide products has helped explain the chemical and structural transformations of the GNO complex in the presence of silicatein (Fig. 4).

The Ga_2O_3 products derived from pyrolysis of GNO and hydrated GNO exhibited an amorphous Ga_2O_3 phase at low and intermediate temperatures ($T < 700$ °C), requiring significant thermal energy for subsequent rearrangement to yield crystalline Ga_2O_3 (Figs. 4a,b). In contrast, the product of base-catalyzed GNO hydrolysis at room temperature was crystalline GaOOH (Fig. 4c). This result demonstrates that the strongly nucleophilic hydroxide ion is capable of readily deprotonating the hydrated precursor more rapidly than occurs under acidic conditions[19] to yield an incompletely condensed crystalline product. Subsequent heat-treatment to 400 °C was sufficient to completely dehydrate GaOOH to yield crystals of corundum, α-Ga_2O_3, as evidenced by as thermal gravimetric analysis/differential thermal analysis data (not shown). The corresponding transformations previously had been seen with powders precipitated from GNO solutions under basic conditions in the presence of urea[20] and in aluminum oxide systems.[21]

The formation of the GaOOH or Ga_2O_3 (spinel) condensation products on silicatein, and the lack of product on non-catalytically active silk and denatured silicatein fibers, implicate enzymatic catalysis, although the pathways of formation differ as a function of reaction conditions. Roy et al.[22] synthesized both α- and γ-phases of Ga_2O_3 at 400 °C from amorphous gallium hydroxide gels. The specific phase that formed was dependent on the rate of thermal treatment, indicating the direct relationship between the metastable phase that is formed and its rate of formation. We observe that the morphology of the Ga_2O_3 formed on the silicatein surface at a low precursor concentration (Figs. 2a,3) closely resembles that of the GaOOH formed on the silicatein surface at a high precursor concentration, suggesting that the Ga_2O_3 may have been formed by topotactic dehydration and condensation of an oxo-hydroxide intermediate. Alternatively, it is possible that dissolution and reprecipitation on the protein surface yield the final oxide product. These observations are related to our finding that two different products, GaOOH and Ga_2O_3, are formed under similar thermodynamic but different kinetic conditions.

Whereas the literature on gallium oxide phase stability is relatively sparse, there are a number of examples of the spinel phase forming at room temperature in kinetically controlled reactions with the analogous iron oxide and aluminum oxide systems. Meldrum et al.[23] synthesized magnetite and maghemite in reactions within the controlled environment of ferritin shells. Yaacob et al.[24] mimicked the bacterial synthesis of magnetite in zwitterionic vesicles. It also is known that γ-Al_2O_3 (spinel) forms as the dehydration product of γ-AlOOH (boehmite), whereas α-AlOOH (diaspore) condenses to form α-Al_2O_3 (corundum).[25] Apparently reflecting a lower crystal interfacial-energy barrier afforded during homogeneous nucleation, γ-Al_2O_3 (spinel) was found to form both by dehydration of γ-AlOOH (boehmite) and via dissolution and reprecipitation of amorphous Al_2O_3 to yield α-Al_2O_3.[26,27] These transformations from diaspore to corundum and boehmite to spinel were shown to be topotactic, taking place without changing the packing order of oxygen atoms.

Silicatein is a member of the enzyme superfamily of catalytic triad hydrolases.[13] Site-directed mutagenesis and biomimetic synthesis studies support the hypothesis that interaction between the essential serine and histidine side chains at the catalytic active site increase the nucleophilicity of the serine oxygen, facilitating its attack and subsequent hydrolysis of silicon alkoxide precursors.[9–11] We suggest that this enhanced nucleophilicity of the enzyme's active-site oxygen similarly facilitates hydrolysis of a hydrated gallium nitrate (the precursor predicted by the PCM to exist under the conditions we employed), with subsequent condensation to form an oxo-hydroxide intermediate at high precursor concentrations. The unique array of additional hydroxyls on the silicatein surface, previously implicated in the templating of silica during biosynthesis,[9] may direct the orientation of an initially formed nanocrystalline gallium oxo-hydroxide via hydrogen-bonding interactions. Such interactions with the silicatein surface may help explain both the preferred orientation of the nanocrystalline product that we observe and the low-temperature formation of the spinel polymorph that otherwise would require $T > 400$ °C. Kinetic control of inorganic crystallization products by organic surfaces has been observed in numerous studies inspired by biomineralization, as reviewed recently by Colfen and Mann.[28] As these authors suggest, the interactions between solute, embryonic clusters, and surfaces can influence not only the particle size and habit of the nucleating crystals, but also the stability of intermediate phases through the lowering of activation energies required for the formation of specific polymorphs and crystal faces by interfacial recognition. Such interfacial control is commonly seen in the kinetically controlled growth of metastable phases of oriented oxides and nitrides that can be stabilized through proper selection of substrates with lattices and interfacial energies matched to those of the overgrowing epitaxial layer.[29]

These results, in concert with our recent observation that silicatein filaments catalyze the synthesis of the anatase phase of TiO_2 from an organic molecular precursor,[12] establish the feasibility of a catalytic route to nanostructurally directed metal oxide semiconductor synthesis at low temperature.

Experimental

Synthesis: Silicatein filaments were purified with minor modifications of the method previously described [12]. Thermal denaturation was accomplished by heating silicatein filaments in a water bath (95 °C) for 1 h. For reactions at high concentration, native and denatured filaments at 2.0 mg mL^{-1} were incubated in 1.6 mL polyethylene centrifuge tubes with 1 mL of a 1.0 M aqueous solution of gallium ni-

ADVANCED MATERIALS

trate (GNO, Alfa Aesar, Ward Hill, MA) for 6 h at 16 °C. The products were collected and washed by centrifugation before analysis. For reactions at low concentration, native and denatured filaments at 0.2 mg mL^{-1} were incubated in 1.6 mL polyethylene centrifuge tubes with 1 mL of a 0.1 M aqueous solution of gallium nitrate for 24 h at 25 °C. The products were collected and washed by centrifugation before analysis. Base-catalyzed synthesis of Ga_2O_3 was accomplished by dissolving 1.82 g (0.005 mol) of GNO in 30 g of water contained in a glass vessel, followed by the addition of 7.24 g (0.06 mol) of concentrated (~29 wt.-%) ammonium hydroxide (NH_4OH). Precipitated product was collected and washed by centrifugation before heat treatment. Hydrated GNO was prepared by dissolving 1.82 g (0.005 mol) of GNO in 50 g of water contained in a glass vessel. The solution was mixed for 1 h, followed by room-temperature vacuum evaporation of the water. The dried powder product was used for further heat treatments. As-received GNO powder was used directly from the container for pyrolysis experiments. Thermal treatments of base-hydrolyzed, hydrated, and as-received GNO powders were conducted by heating 50 mg of starting material in alumina crucibles placed in quartz Schlenk tubes. Heat treatments (10 °C min^{-1}) were carried out in air to temperatures between 200–1000 °C for 1 h.

X-ray Diffraction (XRD), Scanning Electron Microscopy (SEM), and Transmission Electron Microscopy (TEM): Approximately 25 mg of each heat-treated sample was ground (with a silicon-powder internal standard) to a fine powder, placed on a glass microscope slide or a single-crystal (100) silicon wafer, and characterized by X-ray diffraction (Phillips X'Pert; Amsterdam, The Netherlands) using a gonio scan (20°–60°, 0.02° step^{-1}, 5 s step^{-1}; source slit sizes of 1/4° and 1/2°, and detector slit sizes of 1/4° and 0.2 mm). Surface features of Ga_2O_3 powders and Ga_2O_3-coated silicatein filaments were imaged by a cold cathode field-emission scanning electron microscope (SEM; JEOL JSM 6300F, Peabody, MA) equipped with an energy dispersive spectrometer. Specimens were mounted on conductive carbon adhesive tabs (Ted Pella, Inc., Redding, CA) and imaged (at 5 kV or 10 kV) either uncoated (for energy dispersive spectroscopy analysis) or after gold/palladium sputter coating. Energy dispersive spectroscopy (EDS, Oxford Instruments, Palo Alto, CA) was performed in conjunction with SEM to qualitatively determine chemical composition of specimens. Ga_2O_3-coated filaments were imaged with a transmission electron microscope (TEM, JEOL 2000FX) to observe the coating morphologies and obtain structural information via electron diffraction patterns. Lattice fringes were imaged with a high-resolution TEM (HRTEM, JEOL 2010). Both TEMs were operated at 200 kV. TEM specimens were prepared by pipetting a small amount (~20 μL) of filament suspension (in water) onto holey-carbon copper grids (Ted Pella, Inc., Redding, CA). The grids were then dried at 40 °C for 5 min. Samples were imaged at magnifications from 20 000× to 200 000× in the conventional TEM, and from 500 000× to 800 000× in the HRTEM. Selected area electron diffraction (SAED) patterns were obtained at camera distances of 55 cm, 83 cm, and 100 cm. A standard evaporated-aluminum film (lattice constant = 0.4041 nm) was used as a standard to determine the exact camera constants.

Received: May 24, 2004
Final version: September 20, 2004

[1] A. H. Heuer, D. J. Fink, V. J. Laraia, J. L. Arias, P. D. Calvert, K. Kendall, G. L. Messing, J. Blackwell, P. C. Rieke, D. H. Thompson, A. P. Wheeler, A. Veis, A. I. Caplan, *Science* **1992**, *255*, 1098.
[2] S. Mann, *Nature* **1993**, *365*, 499.
[3] S. Weiner, L. Addadi, *J. Mater. Chem.* **1997**, *7*, 689.
[4] A. M. Belcher, P. K. Hansma, G. D. Stucky, D. E. Morse, *Acta Mater.* **1998**, *46*, 733.
[5] D. E. Morse, *Trends Biotechnol.* **1999**, *17*, 230.
[6] S. Mann, *Biomineralization: Principles and Concepts in Bioinorganic Materials Chemistry*, Oxford University Press, New York **2001**, pp. 16–23.
[7] M. Sarikaya, C. Tamerler, A. K. Y. Jen, K. Schulten, F. Baneyx, *Nat. Mater.* **2003**, *2*, 577.
[8] J. Aizenberg, D. A. Muller, J. L. Grazul, D. R. Hamann, *Science* **2003**, *299*, 1205.
[9] K. Shimizu, J. Cha, G. D. Stucky, D. E. Morse, *Proc. Natl. Acad. Sci. USA* **1998**, *95*, 6234.
[10] J. N. Cha, K. Shimizu, Y. Zhou, S. C. Christiansen, B. F. Chmelka, G. D. Stucky, D. E. Morse, *Proc. Natl. Acad. Sci. USA* **1999**, *96*, 361.
[11] Y. Zhou, K. Shimizu, J. N. Cha, G. D. Stucky, D. E. Morse, *Angew. Chem. Int. Ed.* **1999**, *38*, 779.
[12] J. L. Sumerel, W. Yang, D. Kisailus, J. C. Weaver, D. E. Morse, *Chem. Mater.* **2003**, *15*, 4804.
[13] G. Dodson, A. Wlodawer, *Trends Biochem. Sci.* **1998**, *23*, 347.
[14] D. E. Morse, in *The Chemistry of Organic Silicon Compounds*, Vol. 3 (Eds: Z. Rappoport, Y. Apeloig), Wiley, New York **2001**, pp. 805–819.
[15] J. N. Cha, G. D. Stucky, D. E. Morse, T. J. Deming, *Nature* **2000**, *403*, 289.
[16] Y. C. Choi, W. S. Kim, Y. S. Park, S. M. Lee, D. J. Bae, Y. H. Lee, G. S. Park, W. B. Choi, N. S. Lee, J. M. Kim, *Adv. Mater.* **2000**, *12*, 746.
[17] M. Ogita, K. Higo, Y. Nakanishi, Y. Hatanaka, *Appl. Surf. Sci.* **2001**, *175–176*, 721.
[18] J. Livage, M. Henry, C. Sanchez, *Prog. Solid State Chem.* **1988**, *18*, 259.
[19] J. C. Brinker, G. W. Scherer, *Sol–Gel Science: The Physics and Chemistry of Sol-Gel Processing*, Academic, Boston, MA **1990**.
[20] A. C. Tas, P. J. Majewski, F. Aldinger, *J. Am. Ceram. Soc.* **2002**, *85*, 1421.
[21] L. Loffler, W. Mader, *Am. Mineral.* **2001**, *86*, 293.
[22] R. Roy, V. G. Hill, E. F. Osborn, *J. Am. Chem. Soc.* **1952**, *74*, 719.
[23] F. C. Meldrum, B. R. Heywood, S. Mann, *Science* **1992**, *257*, 522.
[24] I. I. Yaacob, A. C. Nunes, A. Bose, *J. Colloid Interface Sci.* **1995**, *171*, 73.
[25] G. Erwin, *Acta Crystallogr.* **1952**, *5*, 103.
[26] R. McPherson, *J. Mater. Sci.* **1973**, *8*, 851.
[27] C. G. Levi, V. Jayaran, J. J. Valencia, R. Mehrabian, *J. Mater. Res.* **1988**, *3*, 969.
[28] H. Colfen, S. Mann, *Angew. Chem. Int. Ed.* **2003**, *42*, 2350.
[29] *Epitaxial Growth* (Ed: J. W. Matthews), Academic, New York **1975**.

pH-Triggered Thermally Responsive Polymer Core–Shell Nanoparticles for Drug Delivery**

By *Kumaresh S. Soppimath*, *Darren Cherng-Wen Tan*, and *Yi-Yan Yang**

Polymeric core–shell nanoparticles have emerged recently as promising colloidal carriers for targeting poorly water-soluble and amphiphilic drugs, as well as genes, to tumor tissues.[1–3] Using these nanoparticles, drug targeting can be

[*] Dr. Y.-Y. Yang, Dr. K. S. Soppimath, Dr. D. C.-W. Tan
Institute of Bioengineering and Nanotechnology
31 Biopolis way, The Nanos, 04-01, 138669 (Singapore)
E-mail: yyyang@ibn.a-star.edu.sg

[**] This work was funded by Institute of Bioengineering and Nanotechnology, Agency for Science, Technology and Research, Singapore. Supporting Information is available online from Wiley InterScience or from the author.

  DOI: 10.1002/adma.200401057